HAL
open science

Atmospheric oxidation in the Mexico City Metropolitan Area (MCMA) during April 2003

T. R. Shirley, W. H. Brune, X. Ren, J. Mao, R. Lesher, B. Cardenas, R. Volkamer, L. T. Molina, M. J. Molina, B. Lamb, et al.

To cite this version:

T. R. Shirley, W. H. Brune, X. Ren, J. Mao, R. Lesher, et al.. Atmospheric oxidation in the Mexico City Metropolitan Area (MCMA) during April 2003. Atmospheric Chemistry and Physics, 2006, 6 (9), pp.2753-2765. hal-00295972

HAL Id: hal-00295972

https://hal.science/hal-00295972v1

Submitted on 18 Jun 2008

HAL is a multi-disciplinary open access archive for the deposit and dissemination of scientific research documents, whether they are published or not. The documents may come from teaching and research institutions in France or abroad, or from public or private research centers.

L'archive ouverte pluridisciplinaire **HAL**, est destinée au dépôt et à la diffusion de documents scientifiques de niveau recherche, publiés ou non, émanant des établissements d'enseignement et de recherche français ou étrangers, des laboratoires publics ou privés.

Atmos. Chem. Phys., 6, 2753–2765, 2006
www.atmos-chem-phys.net/6/2753/2006/
© Author(s) 2006. This work is licensed
under a Creative Commons License.

Atmospheric Chemistry and Physics

Atmospheric oxidation in the Mexico City Metropolitan Area (MCMA) during April 2003

T. R. Shirley[1], W. H. Brune[1], X. Ren[1], J. Mao[1], R. Lesher[1], B. Cardenas[2], R. Volkamer[3], L. T. Molina[3], M. J. Molina[3], B. Lamb[4], E. Velasco[4], T. Jobson[5], and M. Alexander[5]

[1]Pennsylvania State University, University Park, PA, USA
[2]Autonomous Metropolitan University, Mexico City, Mexico
[3]Massachusetts Institute of Technology, Cambridge, MA, USA
[4]Washington State University, Pullman, WA, USA
[5]Pacific Northwest National Laboratory, Richland, WA, USA

Received: 1 July 2005 – Published in Atmos. Chem. Phys. Discuss.: 17 August 2005
Revised: 20 April 2006 – Accepted: 9 June 2006 – Published: 7 July 2006

Abstract. The Mexico City Metropolitan Area (MCMA) study in April 2003 had measurements of many atmospheric constituents, including OH and HO_2. It provided the first opportunity to examine atmospheric oxidation in a megacity in a developing country that has more pollution than typical U.S. and European cities. At midday, OH typically reached 0.35 pptv ($\sim 7\times10^6$ cm^{-3}), comparable to amounts observed in U.S. cities, but HO_2 reached 40 pptv, more than observed in most U.S. cities. The OH reactivity was also measured, even during the highly polluted morning rush hour. MCMA's OH reactivity was 25 s^{-1} during most of the day and 120 s^{-1} at morning rush hour, which was several times greater than has been measured in any U.S. city. Median measured and modeled OH and HO_2 agreed to within combined uncertainties, although for OH, the model exceeded the measurement by more than 30% during midday. OH production and loss, which were calculated from measurements, were in balance to within uncertainties, although production exceeded loss during morning rush hour. This imbalance has been observed in other cities. The HO_2/OH ratio from measurements and steady-state analyses have essentially the same dependence on NO, except when NO was near 100 ppbv. This agreement is unlike other urban studies, in which HO_2/OH ratio decreased much less than expected as NO increased. As a result of the active photochemistry in MCMA 2003, the median calculated ozone production from measured HO_2 reached 50 ppb h^{-1}, a much higher rate than observed in U.S. cities.

Correspondence to: W. H. Brune
(brune@ems.psu.edu)

1 Introduction

Megacities contain not only millions of people but also elevated levels of airborne pollutants. These pollutants are generated by the transportation and industry necessary to support these millions. The fast chemistry that transforms primary pollutant emissions of nitrogen oxides (NO_x) and volatile organic compounds (VOCs) is initiated by reactions of the hydroxyl radical, OH, with VOCs. The subsequent reactions produce the hydroperoxyl radical, HO_2, which reacts with NO to reform OH and create NO_2, resulting in the production of the pollutant ozone (O_3). Low volatility VOCs are also generated, resulting in the formation of secondary organic aerosol mass. Together, OH and HO_2, called HO_x, form a rapid reaction cycle that drives this atmospheric chemistry.

Several field studies that include HO_x measurements have been conducted in urban environments in the United States, including Los Angeles, California (George et al., 1999), Nashville, Tennessee (Martinez et al., 2003), Houston, Texas (Martinez et al., 2002) and New York City, New York (Ren et al., 2003a). Field studies with HO_x measurements have also been conducted in urban air in Europe as well, including Berlin, Germany (Volz-Thomas et al., 2003, and accompanying papers) and Birmingham, United Kingdom (Heard et al., 2004; Emmerson et al., 2005). The Mexico City Metropolitan Area (MCMA), a megacity, has more pollution than any of these other urban environments (Molina and Molina, 2002).

A useful addition to the typical measurement suite for studying atmospheric oxidation is the measurement of OH reactivity, the inverse of the OH lifetime (Kovacs and Brune, 2001; Kovacs et al., 2003). This manuscript describes a method for obtaining OH reactivity measurements even in

the presence of high levels of nitrogen oxides (NO_x). The OH reactivity measurement is particularly useful in two ways. First, by comparing the measured OH reactivity with the calculated OH reactivity, which is the sum of the product of OH reactants and their reaction rate coefficients, the completeness of the measured reactants can be tested (Kovacs et al., 2003; DiCarlo et al., 2004). Second, some properties of atmospheric oxidation chemistry can be tested independently of detailed model oxidation mechanisms. For instance we can test the expected balance between OH production and loss and the dependence of the HO_2/OH ratio on controlling variables such as nitric oxide (NO). We have also shown that in some regions OH reactivity combined with a general knowledge of the VOC speciation is sufficient to model the observed OH and HO_2 with a fidelity that is as good as is obtained in field studies with more frequent measurements of speciated VOCs (Ren et al., 2005, 2006).

OH, HO_2, OH reactivity, and other atmospheric constituents important for studying atmospheric oxidation were measured during the Mexico City Metropolitan Area 2003 (MCMA-2003) study, which was held in the MCMA during April 2003. MCMA is at a high altitude (∼2240 m) near the equator at 19°25′ N latitude. At this high altitude and low latitude, intense solar radiation penetrates to the surface causing active photochemistry. In addition to the radiation, the area's orography, with mountains to the west, east, and south of the metropolitan area, traps pollutants in the basin. As a result, MCMA experiences high pollution levels. This study was an opportunity to develop a better understanding of MCMA's high pollution levels of ozone and secondary particulate matter. It also stretches the envelope of polluted environments that have been studied with a measurement suite that includes measurements of OH and HO_2.

2 Description of the MCMA 2003 study

2.1 Site description

Measurements were made from the roof of the building that houses the National Center of Investigation and Environmental Qualification (CENICA) on the campus of the Autonomous Metropolitan University in Iztapalapa, Mexico City. Iztapalapa lies in the south-central MCMA, due south of the downtown area by ∼7 km. To the west and south of the university are mainly residential areas; to the north and east are several factories and industries.

Northerly (southward) wind generally brings air from the downtown to this site during daytime. The winds from all other directions bring air from the surrounding suburbs to the site. In contrast to mid-latitude megacities, high pollution episodes can occur year-round in the MCMA because the subtropical highs that dominate the weather throughout the year are conducive to active photochemistry. During the winter and spring months, the area is normally under an anticyclone with light winds and clear skies. As a result, strong surface-based inversions usually persisted several hours into the morning. Strong solar heating eventually breaks down the inversion and pollutants then mix into a very deep boundary layer 2–4 km deep. This study was held in April to avoid the wetter summer months (June–September) because clouds and precipitation inhibit strong photochemistry (Molina and Molina, 2002). However, in 2003, the summertime pattern began in April, resulting in frequent clouds and some rain in the afternoon.

2.2 GTHOS (Ground-based Tropospheric Hydrogen Oxides Sensor)

OH and HO_2 were measured by the Penn State Ground-based Hydrogen Oxides Sensor, called GTHOS. A brief description of the measurement technique and instrument is given here; a full description can be found in Faloona et al. (2004). GTHOS measurement of OH and HO_2 is based on FAGE (Fluorescence Assay by Gas Expansion) (Hard et al., 1984). The air sample is drawn through an orifice (1.0 mm diameter) into a low-pressure chamber at a pressure of 4–5 hPa. As the air passes through a laser beam, OH is excited by the laser and then detected at a wavelength near 308 nm. Collisional quenching of the excited state is slow enough at the chamber pressure that the weak OH fluorescence extends beyond the prompt scattering (Rayleigh and wall scattering) and is detected with a time-gated microchannel plate (MCP) detector.

OH is detected in the first of two detection axes. In a second axis, HO_2 is chemically converted to OH by reaction with reagent NO that is added to the flow between the two axes. The resultant OH is then detected by LIF. The laser wavelength is turned on and off resonance with an OH transition every 10 s. The OH fluorescence signal is the difference between on-resonance and off-resonance signals.

GTHOS was calibrated before, during, and after the study using the techniques described in Faloona et al. (2004). The upper-limit of the absolute calibration uncertainty was estimated at ±32% (at the 95% – 2σ – confidence level). The OH detection limit can be defined as twice the standard deviation of the background signal and was 0.01 part per trillion by volume, or pptv, ($\sim 2\times10^5$ cm^{-3}) for a 1-min integration period. The HO_2 detection limit (with 2σ – confidence, 1-min integration time) was estimated to be 0.1 pptv ($\sim 2.0\times10^6$ cm^{-3}).

During the campaign in Mexico City, GTHOS was mounted approximately 18 m above the ground on the third level of a scaffolding tower (Fig. 1). Ambient air was pulled through the system by a vacuum pump that was located directly beneath the measurement tower. The electronics and calibration equipment were housed in an air-conditioned hut that was directly adjacent to the tower.

2.3 TOHLM (Total OH Loss Measurement)

The first-order OH loss rate, called the OH reactivity, was measured with the Total OH Loss Measurement instrument (TOHLM) (Kovacs and Brune, 2001; Kovacs et al., 2003; Di Carlo et al., 2004). It was mounted on the first level of the tower, approximately 14 m above the ground. The inlet hose for TOHLM was mounted just below the inlet of GTHOS on the third level of the tower.

The TOHLM method is analogous to the discharge-flow technique used in laboratory kinetics studies. OH is generated at mixing ratios of a few 10's of parts per trillion by volume (pptv) by ultraviolet light from a mercury lamp. This light photodissociates water vapor, creating OH and H in a nitrogen flow inside a 1-cm diameter movable tube. H rapidly reacts with trace O_2 in the N_2 to form HO_2. This moveable tube is in the center of a 7.5-cm diameter glass flow tube through which ambient air is drawn by a fan with a total sampling flow rate of about 140 l min^{-1} and a residence time of 0.1–0.4 s. The OH is injected through radially drilled holes at the end of the movable tube, mixed turbulently into the air flow, and detected by an OH detector at the end of the flow tube. The detection technique is low-pressure laser induced fluorescence, as is used for GTHOS. OH reacts with trace constituents in the air flow and, as the movable tube is drawn further away from the detector, the observed OH signal decreases.

The OH reactivity, k_{OH}, is the slope of the logarithm of the OH signal, S^{OH}, as function of the time (the distance divided by the velocity) minus the OH loss to the flow tube's walls, k_{wall}:

$$k_{OH} = -\Delta \ln(S^{OH})/\Delta\text{time} - k_{wall} \quad (1)$$

Each decay took 4.3 min, with 20 s at each of 13 steps, 10 s measuring OH plus the background signal and 10 s measuring the background signal. The OH signal decreased by a factor of 10–20 over the 13 steps. The measured OH wall loss rate, k_{wall}, was 1.5±0.4 s^{-1}. This measured value was the same before, during, and after the study. Generally, OH mixing ratios were 10–30 pptv inside the glass tubing.

2.4 TOHLM correction technique

Kovacs et al. (2003) and Ren et al. (2003a) discuss the need to correct OH reactivity measurements for the OH-recycling reaction:

$$HO_2 + NO \rightarrow OH + NO_2 \quad (R1)$$

When levels of NO are below 1 ppbv, the measured decays are generally linear and the slopes correct to within 10% (Kovacs et al., 2003). However, when ambient levels of NO are higher, the decays have concave curvature as HO_2 reacts with the NO to reform OH. In past studies where the TOHLM instrument was used, NO concentrations infrequently reached levels that required significant corrections or measurements

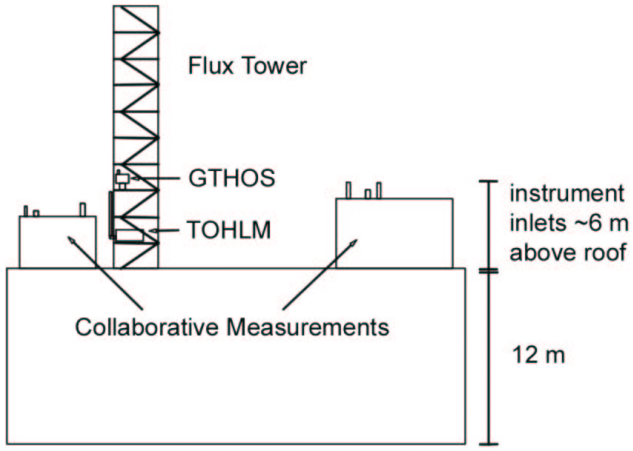

Fig. 1. Schematic of the instruments on the CENICA building roof. Both the Penn State instruments (GTHOS and TOHLM) were on the flux tower with their inlets within 1 m of one another. Collaborative measurements were also taken on the rooftop by other research groups.

from those times were excluded from further analysis. However, in MCMA during rush hour (05:00–09:00 CST), NO exceeded 50 ppbv 40% of the time and 100 ppbv 12% of the time. This frequent contamination of the decays led to a need for a new correction technique that allows k_{OH} to be measured at much higher values of NO than earlier methods (Kovacs et al., 2003).

The rate equation for [OH] is given by the expression:

$$\frac{d[\text{OH}]}{dt} = -k_{\text{OH}}[\text{OH}] + k_{\text{NO+HO2}}[\text{NO}][\text{HO}_2] = -k_{\text{OH}}[\text{OH}] + k_{\text{NO+HO2}}[\text{NO}]\text{R}\,[\text{OH}] \quad (2)$$

where k_{OH} is the OH reactivity (s^{-1}) and R is the measured $[HO_2]/[OH]$ ratio. Assuming that the average value for R can be used for each time step, this expression can be integrated to give the value of [OH] at time step t_1:

$$[\text{OH}]_1 = [\text{OH}]_0 \exp\left(-k_{\text{OH}}(t_1 - t_0)\right) \times \exp(+k_{\text{HO2+NO}}[\text{NO}]\,\text{R}\,(t_1 - t_0)) \quad (3)$$

The desired [OH] value is given by the expression $[OH]_0$ exp(-k_{OH} (t_1-t_0)). Thus the corrected [OH] at time t_1 is given by the expression:

$$[\text{OH}]_1^c = [\text{OH}]_1 \exp\left(-\frac{k_{\text{NO+HO2}}[\text{NO}]\,[\text{HO}_2]_{0,1}\,(t_1-t_0)}{[\text{OH}]_{0,1}}\right) \quad (4)$$

where $[OH]_{0,1}$ and $[HO_2]_{0,1}$ are average concentrations of times 0 and 1. Since the observed OH and HO_2 signals are proportional to [OH] and $[HO_2]$ by the calibration factors, C_{OH} and C_{HO2}, which for TOHLM are the same, the OH signal can be corrected for the first time step by the expression:

$$S_1^c = \exp[-(\Delta S_1/S_{0,1})] \times S_1 \quad (5)$$

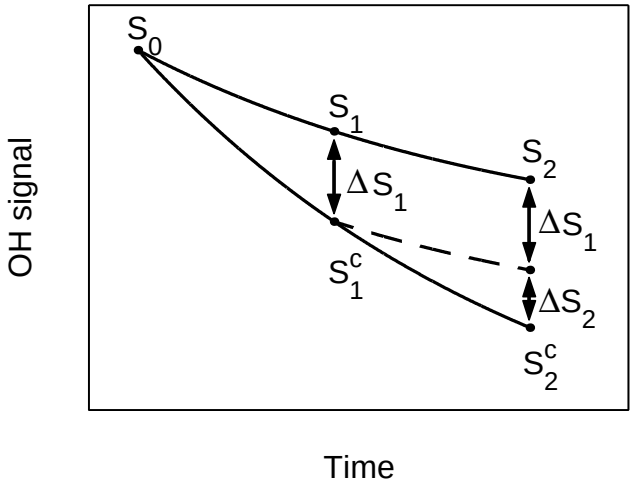

Fig. 2. An example of correcting an OH decay for NO interference. The top curve represents the OH decay with NO interference; the bottom curve is the corrected decay.

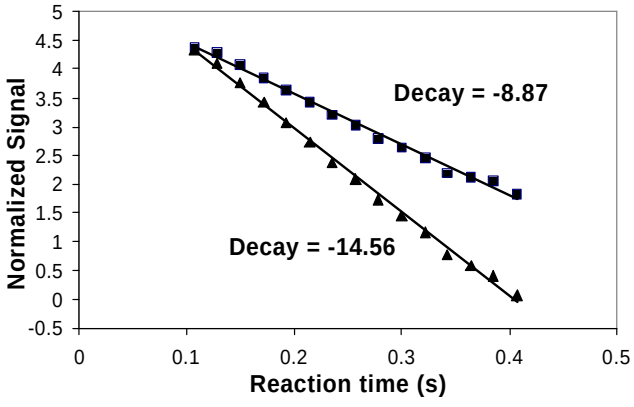

Fig. 3. Laboratory test of the NO correction technique with an average NO concentration of 76.5 ppbv. The top curve represents the original OH decay (squares) with a calculated decay rate of 8.9 s^{-1}; the bottom curve is the corrected OH decay (triangles) with a calculated decay rate of 14.6 s^{-1}. The theoretical decay rate is 14.9 s^{-1}.

where $\Delta S_1 = k_{NO+HO2}$ [NO] $S_{0,1}^{HO2}$ (t_1–t_0) and $S_{0,1}^{HO2}$ is the averaged HO_2 signal for times t_0 and t_1.

In order to correct subsequent points, we must realize that the points are not independent of one another. Points S_1 and S_2 are then scaled by S_1^c by multiplying by S_1^c/S_1, so that the slope between S_1 and S_2 is preserved but the starting point is S_1^c (Fig. 2). The correction given in Eq. (4) is then applied to S_2 and the equation for S_2^c takes the form:

$$S_2^c = \exp[-(\Delta S_1/S_{0,1})] \times \exp[-(\Delta S_2/S_{1,2})] \times S_2 \qquad (6)$$

where $\exp[-(\Delta S_1/S_{0,1})]$ is simply the S_1^c/S_1 that was calculated in Eq. (5). Each subsequent point is calculated in this manner assuring that each point is scaled to the one before it.

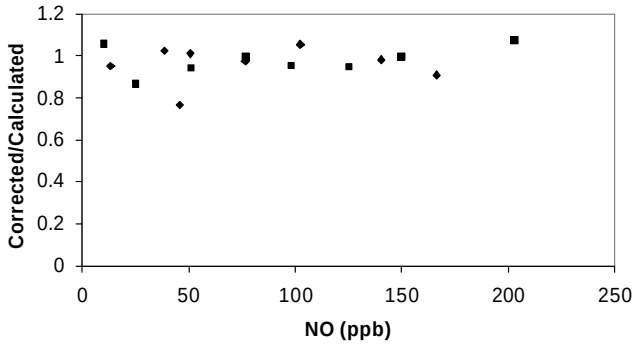

Fig. 4. The ratio of corrected OH decays to the theoretical calculated decays for a wide range of NO values. Decays with just NO (diamonds) and with NO and CO (squares) are both corrected to the expected value with this technique.

This correction technique was tested in the laboratory (Fig. 3). In this example, NO was ∼75 ppbv, a normal rush-hour value for Mexico City. The theoretical calculated decay from the NO and ultra zero air mixture is 14.9 s^{-1}. The uncorrected decay, 8.87 s^{-1}, only 60% of what is calculated, while the corrected decay is 14.6 s^{-1}. Agreement between the calculated and corrected decays is well within the uncertainties of the TOHLM technique and the reaction rate coefficient for OH+NO+M→HONO+M.

This correction technique was used on a wide range of NO concentrations, from 10–200 ppbv (Fig. 4). To ensure that this technique would work when other reactants were present, several different concentrations of CO were added to the instrument along with the NO. In all but one case (with and without the addition of CO) the corrected OH decays were within 15% of the theoretical values. However, the correction factor for decays when NO>100 ppbv grows to a factor of ∼2–3 and becomes more uncertain, since small errors in S^{HO2}/S^{OH} ratio and in NO become more important. Using estimates of the uncertainties in these two terms and considering the number of points used in the decays, we estimate that the uncertainty in the correction is ∼10%, 1σ confidence. Because the correction for 75 ppbv of NO is roughly 1.7, the total absolute uncertainty for the corrected OH reactivity is ±25%, 1 σ confidence, for 75 ppbv of NO.

2.5 Brief descriptions of other measurements

During the MCMA campaign the following ancillary data were continuously measured, with the uncertainties and limit of detection for 10 min in parentheses: O_3 (±15%, 3 ppbv), CO (±15%, 30 ppbv), SO_2 (±20%, 0.5 ppbv), NO (±15%, 0.1 ppbv), NO_2 (±25%, 0.1 ppbv), CH_4 (±5%, 0.2 ppmv), HCHO (±25%, 1 ppbv), HONO (±10%, 0.15 ppbv), temperature, pressure, relative humidity, wind speed, wind direction, and solar ultraviolet radiation. Of these, all but HCHO and HONO were in situ measurements collocated on

the rooftop of the CENICA building with the HO_x measurements. Photolysis frequencies were either measured with a spectroradiometer (±(3–10)%) when available (Volkamer et al., 2005) or calculated with the NCAR TUV transfer model and scaled by measured solar UV radiation (±20%).

HCHO and HONO were made over a 4.4 km path 70 m above the surface (Volkamer et al., 2005). A comparison of other atmospheric constituents that were measured by both in situ and long-path techniques showed the following relationships: $[CO]_{in-situ}=0.96\times[CO]_{long-path}+0.1$ ppmv, with $R^2=0.93$ (Dunlea et al., 2006); $[O_3]_{in-situ}=1.13\times[O_3]_{long-path}-4.6$ ppbv, with $R^2=0.95$ (Dunlea et al., 2006); and $[NO_2]_{in-situ}=1.04\times[NO_2]_{long-path}+8.6$ ppbv, with $R^2=0.81$. These differences are within the measurement uncertainties. Because HCHO has a lifetime similar to O_3 and NO_2 in MCMA, the long-path HCHO measurement should be representative of HCHO at CENICA. For HONO, which is an important OH source and sink mainly during morning rush hour when OH is low, both of its precursor gases OH and NO should generally be fairly uniformly distributed, since NO_2 is. This result is consistent with the conclusion of Dunlea et al. (2006) that "spatial and temporal inhomogeneities were not substantially influencing comparisons of the point sampling and open path instruments." Thus, the long-path measurements of HCHO and HONO and the in situ measurements can be combined in steady state analyses and modeling with only a small increase in the overall uncertainty.

Speciated VOCs were measured during MCMA 2003 by GC-FID automated analysis of samples collected for usually 30 min in stainless steel canisters (Lamb et al., 2004). The measurements were taken at five sites within the MCMA basin with the goal of determining the spatial variability of total VOC carbon and of the fractions of speciated VOCs. These measurements included 11 alkenes, 26 alkanes, 11 aromatics, along with MTBE, ethyl ester, and styrene. The measurement uncertainty was typically ±20%. About 60% of the 120 samples were taken during morning rush hour (05:00–10:00 CST) and most of the remainder during other daylight hours. At CENICA, 75% of the 44 measurements were during morning rush hour. Only two samples were taken at CENICA while the OH reactivity instrument was operating. However, continuous fast total olefin measurements that were made at CENICA every 6 s simultaneously with HO_x and OH reactivity measurements (Velasco et al., 2005) provide another check on the variability of VOC speciation at CENICA.

2.6 Models for analysis of the measurements

Two types of models were used to determine if the measured OH and HO_2 are consistent with the understanding of atmospheric oxidation chemistry in the photochemically active MCMA region. One model is a set of simple algebraic expressions based on steady-state assumptions and using measurements. The other is steady-state photochemical model that is constrained by all the measurements, except OH and HO_2, which are calculated, along with a few other radicals for which there were no measurements.

The Regional Atmospheric Chemistry Mechanism (RACM) (Stockwell et al., 1997) was used to calculate the OH and HO_2 concentrations. Kinetic rate coefficients were updated using the results by Sander et al. (2003). Reactions of O_3 with alkenes have been largely revised to represent latest radical yields suggested by recent experiments (Paulson et al., 1999; Rickard et al., 1999; Fenske et al., 2000). Heterogeneous reactions of HNO_3, SO_3, and N_2O_5 were included in the model. The assumption of steady-state certainly applies to OH, which had a lifetime shorter than 0.1 s and generally to HO_2, which has a lifetime less than a few 10s of seconds.

The model was run with the FACSIMILE software (UES Software Inc). Model input was constrained to the ten-minute average values of O_3, NO, NO_2, CO, SO_2, HCHO, other OVOCs, VOC speciation types found by the process described below, water vapor, temperature, pressure, and photolysis frequencies. The data coverage allowed model calculations only for the period between 14 April and 22 April. OH, HO_2, NO_3, organic peroxyl radicals (RO_2), and other intermediates were calculated. The uncertainty in this RACM model was estimated to be ±45% for OH and ±70% for HO_2, with 2σ confidence. These uncertainties are based on the combined uncertainties of the kinetic rate coefficients (Sander et al., 2003; Stockwell et al., 1997), the measured chemical concentrations, and the measured and calculated photolysis frequencies, as estimated with a Monte Carlo approach (as in Carslaw et al., 1999).

The measurement suite at CENICA was fairly complete, although speciated VOCs were measured infrequently and were not being measured at CENICA when HO_x and OH reactivity were, except for two points. During that time they were being measured at other urban sites. Fortunately, the OH reactivity measurement gives us information about the total amount of VOCs; all that is needed is information about the typical VOC speciation types throughout the day. We employ the same strategy for the MCMA-2003 study that we did for two other recent studies (Ren et al., 2005, 2006). To get the VOC speciation type inputs to the model, the information from the measured OH reactivity was used along with the mean fractions of VOCs types combined from CENICA and three other sites. This combined data set provided full daytime and limited night-time coverage.

What makes this approach feasible is the fairly constant fractions of VOC speciation types despite large variations in the total VOCs. Despite the large variation in total organic carbon, the fraction of VOC speciation types (alkanes, alkenes, aromatics, alkynes, oxygenates) remained the same to less than a factor of two for samples taken from the four most urban sites. For any given time period, the day-to-day

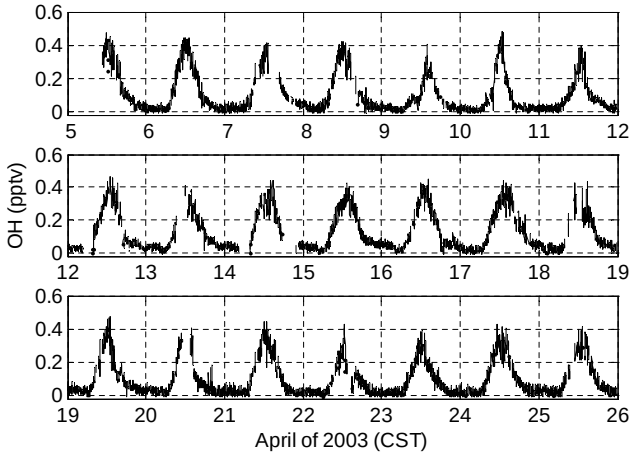

Fig. 5. Time series in CST of all 1-min averaged measured OH (line). Breaks in the data are usually for calibrations. The absolute 2σ uncertainty is ±32%.

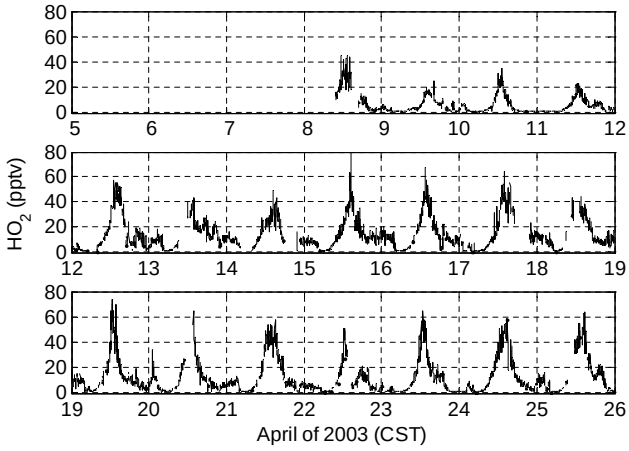

Fig. 6. Time series in CST of all 1-min averaged measured HO_2 (line). Breaks in the data are usually for calibrations. The absolute 2σ uncertainty is ±32%.

scatter in the VOC speciation type measurements for a site was much greater than the differences between sites in the median values for each site. Thus, while plumes and local sources of specific VOCs probably influenced each site, the fraction of VOC speciation types on hour time scales appear to have been uniform to within ±50% for VOC speciation types at the four measurement sites. Additional evidence of this uniformity comes from the fast olefin measurements (B. Lamb, private communication, 2005). The ratio of OH reactivity to fast olefins, when averaged over 30 min, is constant during the day to within ±50%. No matter how this issue is examined, the result is that the 30-min speciation does not generally change more than ±50% throughout the day except for in occasional plumes.

The speciated VOCs were averaged for each half-hour that they were measured and summed into VOC speciation types (e.g., internal alkenes) that the model uses. For the model calculations, the abundance for each VOC speciation type was determined by assigning the same fraction of the measured OH reactivity from VOCs to that VOC speciation type and then calculating the VOC speciation type's abundance from that fraction of the OH reactivity divided by the reaction rate coefficient. This method should work in an average sense. This method has been shown to give good results between measured and modeled HO_x in other studies (Ren et al., 2005, 2006).

Comparisons between HO_x measurements and calculations from the model constrained this way can test the understanding of HO_x photochemical sources and the HO_x dependence on NO and enables the calculation of the instantaneous ozone production rate, $P(O_3)$, if the modeled HO_x is not too sensitive to the chosen VOC speciation types. To test for this sensitivity, a Monte Carlo approach was taken. The fractions of all but one VOC speciation types were randomly varied over the ranges observed in the speciated VOC measurements. The fraction for the VOC speciation type that was not varied was then adjusted so that the sum of the fractions was equal to 1. OH and HO_2 were then calculated. This process was repeated 100 times for each half hour to give a diurnal profile of the range of calculated OH and HO_2. This method gives a good assessment of the sensitivity of the modeled OH and HO_2 to the uncertainties in the VOC speciation.

3 Results and discussion

MCMA 2003 was an excellent opportunity to study the atmospheric chemistry of a megacity that has improving air quality but still more air pollution than a typical U.S. or European city. A goal of MCMA 2003 was a better understanding of the sources and chemical transformations of MCMA's air pollution.

3.1 OH and HO_2: measured values

OH was measured on 21 days in Mexico City from 5 April to 26 April 2003 (Fig. 5); HO_2 was measured on 18 days from 8 April to 26 April 2003 (Fig. 6). The NO addition to the HO_2 axis was deliberately delayed so that any potential interference that it might cause and OH interference could be detected as a change in the OH measurement. No change was detected. OH was fairly consistent from day-to-day, with midday peak values of 0.25–0.4 pptv ((5–8)$\times 10^6$ cm^{-3}). The effects of clouds on OH production can be seen in the reduction in OH on several afternoons. Variability was greater for HO_2 than for OH. Peak HO_2 varied from 15 pptv ($\sim 3\times 10^8$ cm^{-3}) to 60 pptv ($\sim 12\times 10^8$ cm^{-3}).

The HO_2 peak is narrower than the OH peak and is shifted one hour later. HO_2 persisted at ~5 pptv (0.5 to 20 pptv) during the night. HO_2 has a diurnal profile that peaked at

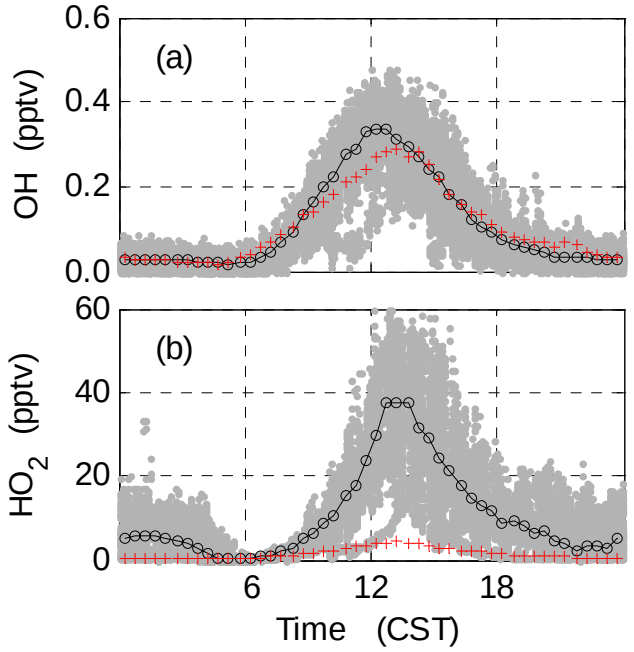

Fig. 7. Diurnal variation of OH and HO_2 for MCMA between 11 April and 21 April. **(a)**: Measured OH in MCMA (solid line) and in NYC (plusses); **(b)**: measured HO_2 in MCMA (solid line) and NYC (plusses). Gray dots are individual MCMA measurements.

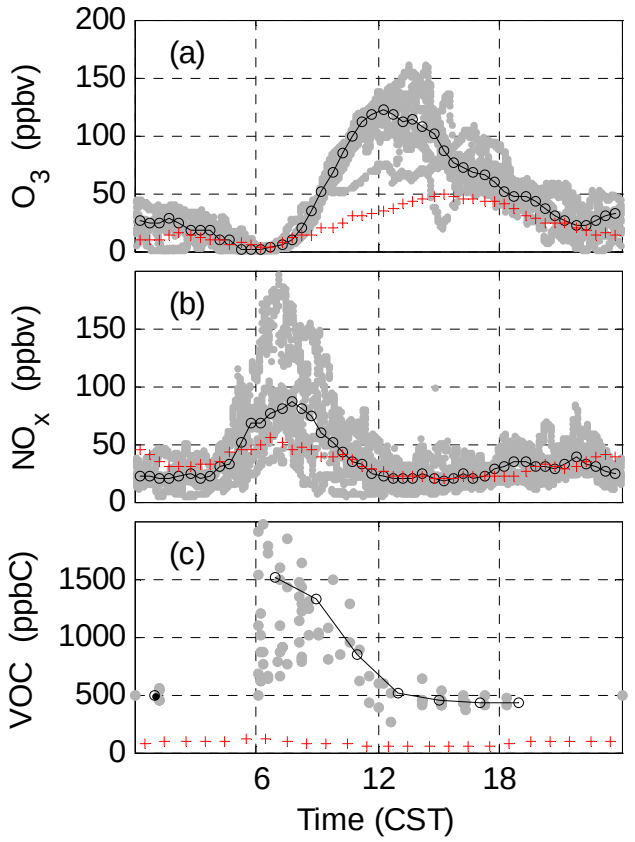

Fig. 8. Diurnal variation of pollutants. **(a)**: Median ozone in MCMA 2003 (solid line) and NYC 2001 (plusses). **(b)**: Median NO_x in MCMA 2003 (solid line) and NYC 2001 (plusses). Gray dots are individual MCMA measurements. **(c)**: Median VOCs from 4 sites in MCMA 2003 (solid line) and NYC 2001 (plusses).

~40 pptv at 13:00, and decreased to less than 0.5 pptv at sunrise, when HO_x production was just beginning to increase but when copious rush-hour NO effectively scavenged HO_2.

The OH and HO_2 diurnal cycles become more distinct when OH and HO_2 are plotted as a function of time-of-day (Figs. 7a and b). The median OH peaks at 0.35 pptv ($\sim 7\times10^6$) cm^{-3} at local noon. The nighttime values ranged from 0.05 pptv ($\sim 1\times10^6$ cm^{-3}) to below the detection limit (0.01 pptv or 2×10^5 cm^{-3}). The median HO_2 peaks at 37.2 pptv and falls off rapidly to less than a few pptv at night, with a minimum at morning rush hour, when NO is rapidly converting HO_2 to OH and NO_2 is rapidly converting OH to HNO_3.

3.2 Comparison between MCMA 2003 and NYC 2001

The comparison of the observations at MCMA to those in U.S. urban areas is also instructive because most U.S. cities are more advanced in their efforts to reign in air pollution than MCMA is. We compare our MCMA observations to our observations taken in New York City (NYC) in July 2001 (Ren et al., 2003a, b). New York City provides a good comparison because it too is a megacity, but is one with more advanced pollution abatement efforts. The measurements in New York City (NYC) were part of PMTACS-NY (PM2.5 Technology Assessment and Characterization Study-New York), which was held Queens, NY during July 2001. Characteristics of MCMA 2003 and NYC 2001 (Table 1) are discussed and shown in the next paragraphs and figures.

Ozone was significantly greater in MCMA 2003 than in NYC 2001 (Fig. 8a). The median MCMA O_3 peak of 115 ppbv was twice that of NYC. The maximum value occurred closer to local noon by about 2 h in MCMA than in NYC, suggesting more active morning photochemistry (Volkamer et al., 2005). Nighttime values were similar in the two locations, with minimum ozone at morning rush hour. In both studies, the observed ozone was less than usual due to atypical weather conditions. In NYC during summer 2001, sea breezes were more frequent than usual, bringing cleaner air from the Atlantic Ocean over the site in Queens. In MCMA during April 2003, the typical summer pattern with afternoon clouds and rain set up early.

Ozone production depends on both NO_x and VOCs. NO_x was significantly greater in MCMA than in NYC only during morning rush hour (Fig. 8b), when, MCMA's median NO_x peaked at 86 ppbv, about 1.6 times the median peak for NYC's NO_x. During the afternoon, both cities had about 20 ppbv of NO_x. Nighttime NO_x was typically 20–35 ppbv

Table 1. Median photochemical characteristics of New York City (NYC), July 2001, and Mexico City Metropolitan Area (MCMA), April 2003.

Median Properties of NYC 2001 & MCMA 2003		
median characteristic	NYC	MCMA
2004 population (10^6)	22	22
total daily J(O^1D)	0.59	0.81
peak NO_x (ppbv)	54	86
peak CO (ppbv)	590	2600
peak O_3 (ppbv)	48	115
OH reactivity kOH (s^{-1})	20	33
kOH from NO_x (%)	42	12
kOH/VOC (s^{-1} $ppbC^{-1}$) VOC (pptv)	0.02	0.07
peak OH (ppbv)	0.28	0.35
peak HO_2 (ppbv)	4.2	37.2

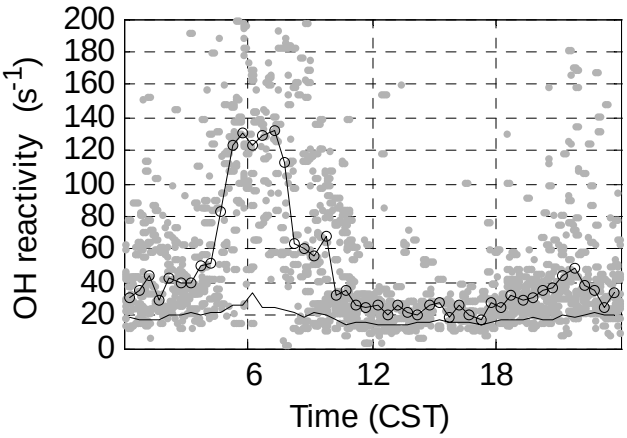

Fig. 9. Diurnal variation of median measured OH reactivity in MCMA 2003 (connected circles) and NYC 2001 (solid line). Gray points are individual MCMA measurements. The maximum absolute 1σ uncertainty is ±25% during morning rush hour and ±15% otherwise.

in both cities. In MCMA, the total VOC abundance differed by a factor of 10 for the four different urban sites and varied a factor of 5 during the day at any site (Fig. 8c). The median value for MCMA 2003 was 1230 ppbC; the median value for NYC 2001 was 80 ppbC. Thus, while MCMA and NYC had NO_x values different by no more than a factor of two, the big difference was the VOCs, which were about 15 times larger in MCMA than in NYC.

It should be noted that the comparison of surface concentrations distorts the differences in NO_x and VOC emissions. The midday mixed layer for MCMA was typically 3–4 km above the surface, while the mixed layer for NYC was typically 1 to 1.5 km. Because the MCMA mixed layer is greater by about a factor of two or three, MCMA's emissions were substantially greater for both NO_x and VOCs than NYC's were.

In MCMA, the OH reactivity, k_{OH}, had a large peak of $\sim$120 s^{-1} during morning rush hour, 25 s^{-1} during midday, and $\sim$35 s^{-1} at night (Fig. 9). This diurnal behavior is similar to that of NO_x, which is consistent with a large transportation source of both OH reactivity and NO_x. This behavior contrasts with the OH reactivity in NYC, which was typically 20 s^{-1} the entire time, with a only small increase during morning rush hour (Fig. 9). The MCMA morning peak is about 5 times what was found in NYC.

During MCMA 2003, only two VOC samples were taken at CENICA while the OH reactivity instrument was operating. For these two samples, the measured OH reactivity was 1.3 times the calculated OH reactivity, within the combined 2σ uncertainties. However, with very little overlap between the measured OH reactivity and the measured VOCs, it is not possible to examine the completeness of the measured VOCs and other OH reactants.

The fraction of OH reactivity due to VOCs can be calculated by subtracting the reactivity due to NO, NO_2, O_3, SO_2, HO_2, CH_4, HONO, HCHO, and other continuously measured species. From this analysis, for the OH reactivity in MCMA, 12% was due to NO_x, 7% to CO, 4% to HCHO. This values are consistent with 72% of the OH reactivity coming from VOCs, as was calculated by the model. In contrast, for OH reactivity in NYC, 42% was due to NO_x, 12% to CO, and 11% to OVOCs, 40% of which is due to HCHO, while VOCs contributed $\sim$20%. Examining the OH reactivity due only to VOCs, the median ratio of the OH reactivity per ppbC of VOCs was $\sim$0.02 s^{-1} $ppbC^{-1}$ in MCMA, but was $\sim$0.07 s^{-1} $ppbC^{-1}$ in NYC. This difference in the OH reactivity per VOC carbon is not surprising considering the large abundances of less-reactive alkanes, mainly propane, found in MCMA compared to NYC (Mugica et al., 2003; Parrish et al., 1998; Lamb et al., 2004).

The observed OH in MCMA is similar to the observed OH in NYC, despite the large differences in OH reactivity (Fig. 7a). The peak value in New York City is shifted 2 h past solar noon, but at 0.28 pptv is only 20% lower than the average peak OH for MCMA.

The HO_2 in MCMA was generally eight times larger than the HO_2 was in NYC (Fig. 7b). This large difference results from the large difference in the HO_x sources, although the photolysis frequencies were only 40% greater than in MCMA than NYC. A big difference was the greater amount of HCHO in MCMA. It peaks at $\sim$20 ppbv in the morning (R. Volkamer, private communication, 2005), represents about 40% of the HO_x source, and was about 15 times larger in MCMA than in NYC during midday. Ozone, which is twice as large in MCMA as in NYC, also contributed to the difference in HO_x. The HO_x sink, which was predominantly the reaction $OH+NO_2+M \rightarrow HNO_3+M$, was comparable in the two cities except during morning rush hour, when it was twice as large in MCMA.

These MCMA HO_x measurements are a good example of the buffering effects of the OH production and loss processes. Over the course of the study, HO_2 peak values varied greatly from day-to-day, indicating dramatic changes in HO_x sources, but OH peak values remained relatively unchanged, as can be seen by comparing Figs. 5 and 6 and by comparing the MCMA and NYC median HO_x values in Fig. 7. That HO_2 is much more sensitive to HO_x sources and sinks than OH suggests that HO_2 must be measured along with OH to really test and understand the radical chemistry.

3.3 OH and HO_2: modeled values

Model calculations of OH and HO_2 were made in the period between 14 April and 22 April, when the measurement suite was the most complete. The measured and modeled OH and HO_2 are compared in the median because of the potential uncertainty introduced by the somewhat limited speciated VOC measurements at CENICA while OH and HO_2 were being measured. However, it is interesting that the comparison of individual 10-min averaged data yields the following relationships between measured and modeled values: $(OH)_{model}=1.2\times(OH)-0.008$ pptv, with $R^2=0.80$ and $(HO_2)_{model}=0.90\times(HO_2)+0.98$ pptv, with $R^2=0.64$, both within the measurement uncertainties. This good agreement between model and measurement, even for 10-min comparisons, indicates that either the fraction of VOC speciation types is not changing significantly or the changes that are occurring in VOC speciation types are not significant for OH and HO_2 modeling or both.

The median modeled and measured OH and HO_2 show similar behavior (Figs. 10a, b). The measured-to-modeled OH ratio is 1.07 during morning rush hour (05:00–09:00 CST), 0.77 during midday (10:00–14:00 CST), and 1.07 at night (20:00–04:00 CST) (Fig. 10a). The measured-to-modeled HO_2 ratio is 1.17 during morning rush hour (05:00–09:00 CST), 0.79 during midday (10:00–14:00 CST), and 1.25 at night (20:00–04:00 CST) (Fig. 10a). Median measurements and models agree with uncertainties for both OH and HO_2.

Using a Monte Carlo approach to vary the VOC speciation over the range of values observed in MCMA, as described in Sect. 2.6, median modeled OH and HO_2 are compared to the median observations (Figs. 10c, d). Close inspection reveals that the entire range of the modeled OH results is ±15% during midday and ±45% for evening and night; the entire range of the modeled HO_2 results is ±15% during the day and ±60% during the evening and night. These ranges are less than the OH 2σ modeling uncertainty of ±45% for OH and ±70% for HO_2. Because the uncertainties are independent, the total model uncertainty increases insignificantly during the day and about 35% during the evening and night. The additional uncertainty induced by the observed factor-of-two variation in the VOC speciation types does not alter any of our conclusions about the comparisons between measured and modeled OH and HO_2 for MCMA.

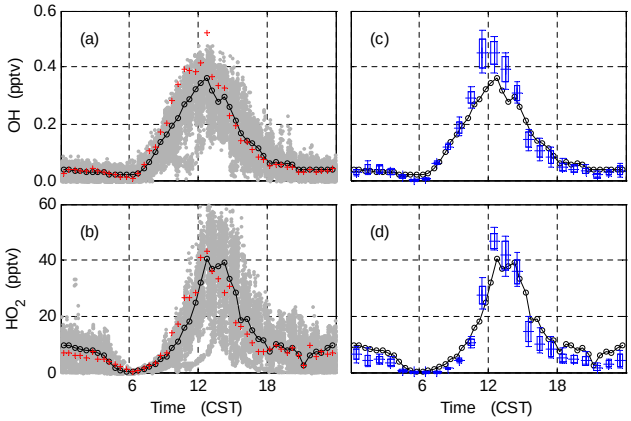

Fig. 10. Diurnal variation of OH and HO_2 for MCMA between 11 April and 21 April. **(a)**: OH – measured (solid line) and modeled (plusses); **(b)**: HO_2 – measured (solid line) and modeled (plusses); **(c)** OH – measured (solid line) and modeled with Monte Carlo treatment of speciated VOC fractions, where boxes define standard deviations and error bars define maximum and minimum values; **(d)** HO_2 – measured (solid line) and modeled with Monte Carlo treatment of speciated VOC fractions, where boxes define standard deviations and error bars define maximum and minimum values. Gray dots are individual MCMA measurements. For OH, the absolute 2σ uncertainty is ±32% for the measurements and ±45% for the model. For HO_2, the absolute uncertainty is ±32% for the measurements and ±70% for the model.

Thus, both the VOC speciation types were not changing significantly and the observed factor-of-two changes in VOC speciation types are not significant for modeling OH and HO_2 in MCMA. This result should not be too surprising. The exception is, of course, the occasional plume of air from an atypical source, but even models that ingest hourly VOC samples will likely not model OH and HO_2 correctly unless the plume a stable for more than an hour. Thus, although knowing the typical VOC speciation is important, the greatest changes in VOC that occurred in MCMA were in the VOC abundance, which the OH reactivity measurement tracked well.

3.4 The HO_2/OH ratio as a function of NO

Examining the HO_2/OH ratio tests the fast photochemistry that cycles HO_x between these OH and HO_2. The HO_2/OH ratio is approximately given by the equation:

$$\frac{[HO_2]}{[OH]} = \frac{k_{OH}}{k_{HO2+NO}[NO] + k_{HO2+O3}[O_3] + P(OH)_{primary}/[HO_2]} \quad (7)$$

where $P(OH)_{primary}$ is the OH produced by every source except cycling through HO_2.

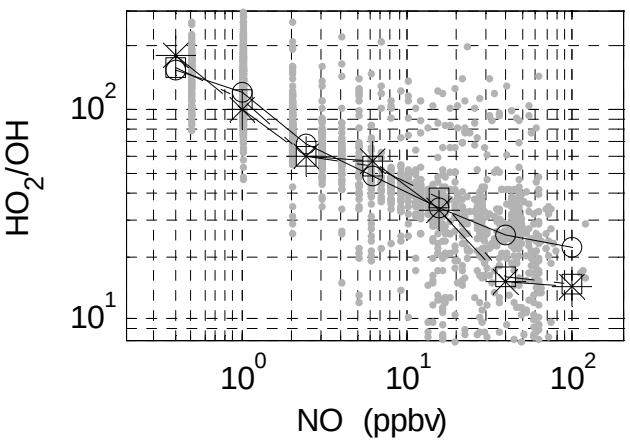

Fig. 11. Dependence $[HO_2]/[OH]$ ratio with NO. Measurements (circles and line), modeled using Eq. (7) (squares and dash-dot line), and modeled using RACM (stars and dashed line) are shown. Gray dots are individual 10-min measurements. Lines are added to aid comparison.

For MCMA 2003, midday HO_2/OH was typically 120, with low values of 10–15 during morning rush hour and high values of 200 at night (Fig. 11). This behavior is quite different from New York City, where the ratio was typically ∼15 at all times (Ren et al., 2003a). The difference in the midday HO_2/OH ratio between MCMA and NYC is due to differences in midday NO, which was typically less than 1 ppbv in MCMA but 5 ppbv or higher in NYC, and the midday OH reactivity, which in MCMA was typically 1.5 times that in NYC. Typically, the reaction of HO_2 with NO is more than 10 times larger than either the reaction of HO_2 with O_3 or with the primary OH production divided by $[HO_2]$. Equation (7) can often be approximated by the expression:

$$\frac{[HO_2]}{[OH]} \approx \frac{k_{OH}}{k_{HO2+NO}[NO]} \quad (8)$$

Increasing the numerator in Eq. (8) by 1.5 and decreasing the denominator by ∼5 provides the difference of eight in the MCMA and NYC HO_2/OH ratios.

The measured HO_2/OH ratios display the same dependence on NO as the ratio obtained from the steady-state expression in Eq. (7) for NO between 1 and 100 ppbv and from the model (Fig. 10). The steady-state expression, which is calculated only from measured quantities, shows the same NO-dependence for HO_2/OH as the model does. The observed and modeled ratios vary approximately as the 1/2 power of NO, whereas an NO power dependence of 1 to 2 is expected. This less-than-theory power dependence comes from the co-emission with NO of atmospheric constituents that react with OH, thus increasing HO_2. The measured ratio is higher than the modeled ratio when NO exceeds 20 pptv but only by less than a factor of two.

While such good agreement between the measured and modeled ratio is expected, this behavior has not been observed in some other urban areas. Typically, the measured HO_2/OH has had a much shallower slope with respect to NO than the modeled ratio does, resulting in the measured ratio being as much as ten times larger than the modeled ratio for NO exceeding 10 ppbv (Ren et al., 2003; Martinez et al., 2003; Emmerson, 2005). Neither the reason for the poor agreement in other urban areas nor the reason for the different behavior in MCMA are currently understood.

3.5 OH production and loss

MCMA's OH reactivity of 20 s^{-1} during most of the day and 120 s^{-1} at morning rush hour implies OH lifetimes of 50 ms to 8 ms. This lifetime is much shorter than the time scales for other processes, including mixing of emissions, changes in photolysis, and other chemistry. As a result, the OH production should equal the OH loss:

$$\begin{aligned} P(OH) &= 2J_{O3}f[O_3][H_2O] \\ &\quad + J_{HONO}[HONO] + k_{NO+HO2}[NO][HO_2] \\ &\quad + k_{O3+VOC}[O_3][VOC] + \text{other smaller terms} \\ &= k_{OH}[OH] = L(OH) \end{aligned} \quad (9)$$

where f is the fraction of $O(^1D)$ that is produced from O_3 photolysis and reacts with H_2O to produce OH. The OH loss is determined simply from the product of [OH] and the OH reactivity, both of which are measured. Over 80% of the OH production is controlled by $[HO_2]$ and [NO], both of which are measured. The first three OH production terms were calculated from measurements; the fourth term, OH production from O_3 and alkenes, was taken from model results and was less than 5±3% of the total.

P(OH) and L(OH) are in balance to within the combined 2σ uncertainties of the OH production and loss terms (Fig. 12). The difference L(OH)–P(OH) should be zero for the entire day, but it is actually slightly negative during morning rush hour (05:00–09:00 CST), implying greater-than-expected production. Smaller L(OH)–P(OH) differences at morning rush hour were observed in Nashville (Martinez et al., 2003) and in New York City (Ren et al., 2003a).

These differences at morning rush hour are not beyond the measurement uncertainties, and yet they are persistent from study to study. For MCMA between 07:00 and 08:00 CST, OH production is double the OH loss. Previous attempts to explain these differences with instrumental artifacts for HO_2 have failed (Ren et al., 2004); however, it is possible that our laboratory tests of the correction algorithm for HO_2+NO→OH+NO_2 do not apply to MCMA air, with its more complex composition. This explanation, however, seems unlikely.

If the measurements are correct, then the imbalance in the OH production and loss at morning rush hour indicates problems with known urban photochemistry. We are left with the conclusion that some aspect of the HO_x–NO_x photochemistry may need re-examination. One solution would be that

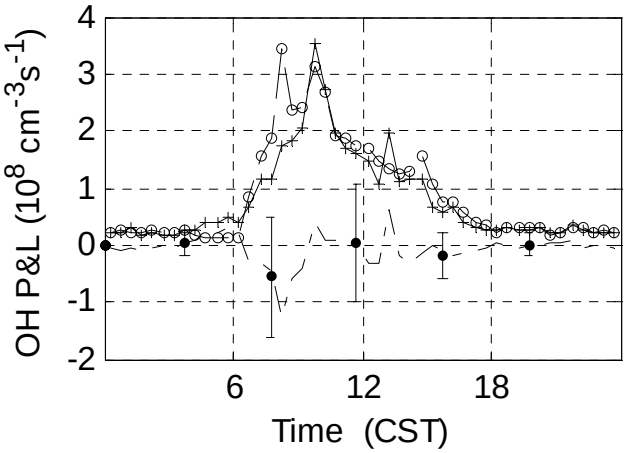

Fig. 12. Diurnal variation of the median OH production (circles) and median loss (plusses), and median loss – production (dot-dash line) for MCMA. Error bars are 2 σ absolute uncertainty on OH loss – OH production.

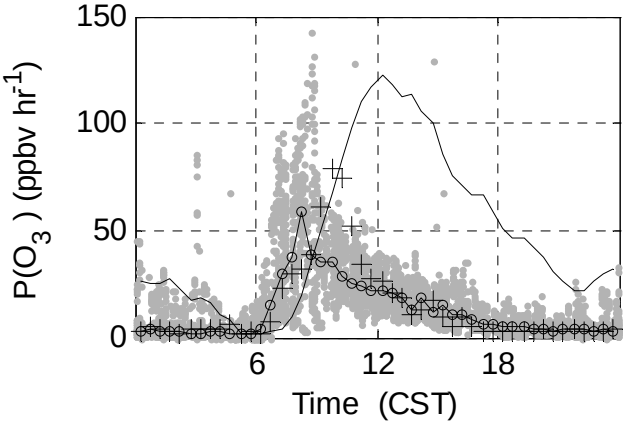

Fig. 13. Diurnal average of instantaneous photochemical ozone production (P(O_3)). 30-min median P(O_3) from measured HO_2 (circles) is compared to 30-min median P(O_3) from modeled HO_2 (plusses). Median observed ozone (ppbv) is plotted as a solid line to illustrate the lag between the time of maximum P(O_3) and the time of maximum O_3. Gray dots are individual 30-min median P(O_3) from measured HO_2.

some products of the reaction HO_2+NO are not OH+NO_2. Instead, this imbalance provides evidence that some of the HO_2+NO reaction results either in HO_x removal or couples with another reaction that rapidly cycles back to HO_2 without going through OH. The uncertainty in the MCMA measurements does not allow us to distinguish between HO_x removal or rapid cycling. A study of the imbalance in the NO_x photostationary state led Volz-Thomas et al. (2003) to a similar and possibly related conclusion: an unknown process is converting NO to NO_2 without resulting in ozone production.

3.6 Instantaneous O_3 production

The net instantaneous O_3 production is in some ways a better indicator of the connection between ozone precursors and ozone than is the ozone mixing ratio itself (Kleinman et al., 2000). Instantaneous ozone production is not subject to the uncertainties in physical processes like horizontal advection, planetary boundary layer height changes, entrainment of free-tropospheric air, and dry deposition. On the other hand, because it does not take these physical processes into account, it is a poor indicator of the actual ozone mixing ratios that will occur. Nevertheless, it does provide insight into the chemical processes that create ozone at the CENICA site.

The net instantaneous photochemical O_3 production can be calculated by the equation:

$$\mathrm{P(O_3)} = k_{\mathrm{HO2+NO}}[\mathrm{NO}][\mathrm{HO_2}] + \Sigma k_{\mathrm{RO2i+NO}}[\mathrm{NO}][\mathrm{RO_{2}}_i] - k_{\mathrm{OH+NO2+M}}[\mathrm{M}][\mathrm{NO_2}][\mathrm{OH}] - \mathrm{P(RONO_2)} \quad (10)$$

For urban environments like MCMA, including the NO_2 lost to HNO_3 or organic nitrate ($RONO_2$) formation can offset ~10% of the ozone production and must be included. If P(O_3) is calculated only from the measured quantities HO_2, NO, OH, and NO_2, then only the first and the third terms are retained. This reaction, of course, assumes that all of HO_2+NO forms OH+NO_2 and that NO_2 is photolyzed to produce ozone.

The median P(O_3) calculated from measured HO_2 peaked at 48 ppbv h^{-1}, while P(O_3) calculated from modeled HO_2 peaked at 86 ppbv h^{-1} (Fig. 13). Both peaks are broad and achieve maximum values near 10:00 CST. Peak values on some days were greater than 100 ppbv h^{-1}.

The NO_x peak at morning rush hour is mainly due to fresh NO emissions (Fig. 8). Beginning at about 05:00 CST, O_3 was drawn down by the reaction with NO to form NO_2, but the sum of NO_2+O_3 remained relatively constant. As P(O_3) began to increase at 06:00 CST, NO_2+O_3 began to increase, but more than 90% of the produced O_3 was partitioned into NO_2 by reaction with NO. O_3 did not begin to really rise until about 07:30 CST, when NO had fallen to half its peak value and J(NO_2) had climbed to 16% of its peak value. Thus, the sum of NO_2+O_3 rose along with P(O_3), while the O_3 rise appears to have been delayed by about 1.5 h (Fig. 13).

In New York City, the median mid-morning P(O_3) from HO_2 was 12 ppbv h^{-1}, peaking at 11:00 EDT. On a few days, P(O_3) from HO_2 reached as high as 50 ppbv h^{-1}, but on many days, its peak value was less than 10 ppbv h^{-1}. This ozone production rate from HO_2 is about five times smaller than that observed in MCMA. The difference in the measured HO_2 in MCMA and NYC causes the difference in P(O_3).

The cumulative daily surface ozone production from HO_2 at the CENICA site was calculated to be 319 ppbv by measurement. To relate cumulative surface ozone production to the observed ozone requires the knowledge of the temporal and spatial variations of P(O_3) and O_3 throughout the MCMA, both horizontally and vertically.

4 Summary and conclusions

The MCMA 2003 study stretched the envelope of the pollution levels for which a set of atmospheric measurements that included OH and HO_2 have been obtained. We summarize several conclusions from this study.

First, the measurements of OH. HO_2, and OH reactivity are the first for a megacity in the developing world. This study shows that high-quality measurements are possible in an environment that is more polluted than typical U.S. and European cities.

Second, even in an environment with such high loadings of NO_x and VOCs, steady-state photochemical models are generally able to simulate the median measured OH and HO_2. Monte Carlo analyses of the VOC speciation types confirms that the sparse speciated VOC measurements in CENICA only slightly degraded the comparison between measurement and model for OH and HO_2. The agreement between the measured and modeled HO_x is as good as or better than that obtained in other urban environments (George et al., 1999; Martinez et al., 2003; Ren et al., 2003b; Heard et al., 2004).

Second, while the OH sources and sinks are both substantially increased over those in U.S. cities, the resulting OH is similar to that observed in U.S. cities. Not so for HO_2, which was greater in MCMA than in U.S. cities and is thus directly responsible for the differences seen in the ozone levels between MCMA and U.S. cities.

Third, the OH reactivity was higher than we have observed in any other outdoor environment, reaching more than $120\,s^{-1}$ in morning rush hour. Our correction scheme for HO_2+NO→OH+NO_2 allows OH reactivity measurements to be made in much more polluted environments than before. Because of the poor overlap between speciated VOC and OH reactivity measurements at CENICA, the data are insufficient to rule out the possibility that the measured OH reactivity is as much as 30% greater than the calculated OH reactivity, similar to our measurements in Nashville (Kovacs et al., 2003) and to other measurements in Tokyo (Sadanaga et al., 2004).

Fourth, a surprising result is the good agreement as a function of NO between the HO_2/OH ratio that is measured and the ratio from a measurement-based steady-state model and a photochemical point model, although the measured ratio is two times greater than the steady-state analysis ratio when NO exceeds 20 ppbv. This agreement is better than we have seen in any other environment where NO exceeded a few ppbv. The difference between these other urban areas and MCMA is not particularly the NO_x abundance, which is similar to that in New York City, but instead is the large amounts of VOCs that result in high OH reactivities.

Fifth, the balance between OH production and loss is generally consistent with the expected OH steady-state balance. A possible exception is during morning rush hour when OH production exceeds OH loss by as much as a factor of two. While the differences are not statistically significant, they do bear watching because they suggest errors in HO_x–NO_x photochemistry.

Finally, the combination of high OH reactivity, abundant sunlight, and NO_x at morning rush hour jump starts ozone production, which from HO_2 alone reached $\sim$50 ppbv h^{-1} by mid-morning. Similar results are found by R. Volkamer (private communication, 2005). Had the meteorological conditions not produced afternoon clouds, occasional rain, and below normal temperatures, midday ozone levels would have been greater.

Acknowledgements. We thank the entire MCMA team for the support they provided us during the MCMA 2003 campaign and for the stimulating discussions at the science workshop. We also thank our colleagues for the use of their data for our model calculations. This work was supported by NSF Atmospheric Chemistry grants (ATM-0209972 and ATM-308748) and the Comisión Ambiental Metropolitana of Mexico. R. Volkamer acknowledges the Henry and Camille Dreyfus Foundation for a Dreyfus postdoctoral fellowship.

Edited by: A. Hofzumahaus

References

Carslaw, N., Jacoba, P. J., and Pilling, M. J.: Modeling OH, HO_2, and RO_2 radicals in the marine boundary layer, 2. Mechanism reduction and uncertainty analysis, J. Geophys. Res., 104, 30 257–30 273, 1999.

Di Carlo, P, Brune, W. H., Martinez, M., Harder, H., Lesher, R., Ren, X, Thornberry, T., Carroll, M.A., Young, V., Shepson, P. B., Riemer, D., Apel, E., and Campbell, C.: Missing OH reactivity in a forest: Evidence for unknown reactive biogenic VOCs, Science, 304, 722–725, 2004.

Dunlea, E. J., Herndon, S. C., Nelson, D. D., Volkamer, R. M., Lamb, B. K., Allwine, E. J., Grutter, M., Ramos Villegas, C. R., Marquez, C., Blanco, S., Cardenas, B., Kolb, C. E., Molina, L. T., and Molina, M. J.: Technical note: Evaluation of standard ultraviolet absorption ozone monitors in a polluted urban environment, Atmos. Chem. Phys. Discuss., 6, 2241–2279, 2006, http://www.atmos-chem-phys-discuss.net/6/2241/2006/.

Emmerson, K. M., Carslaw, N., Carpenter, L. J., Heard, D. E., Lee, J. D., and Pilling, M. J.: Urban Atmospheric Chemistry during the PUMA Campaign, 1: Comparison of Modelled OH and HO_2 Concentrations with Measurements, J. Atmos. Chem., 52, 143–164, 2005.

Faloona, I. C., Tan, D., Lesher, R. L., Hazen, N. L., Frame, C. L., Simpas, J. B., Harder, H., Martinez, M., Di Carlo, P., Ren, X., and Brune, W. H.: A laser induced fluorescence instrument for detecting tropospheric OH and HO_2: Characteristics and calibration, J. Atmos. Chem., 47, 139–167, 2004.

Fenske, J. D., Hasson, A. S., Paulson, S. E., Kuwata, K. T., Ho, A., and Houk, K. N.: The pressure dependence of the OH radical yield from ozone-alkene reactions, J. Phys. Chem. A, 104, 7821–7833, 2000.

George, L. A., Hard, T. M., and O'Brien, R. J.: Measurement of free radicals OH and HO_2 in Los Angeles Smog, J. Geophys. Res., 104, 11 643–11 655, 1999.

Hard, T. M., O'Brien, R. J., Chan, C. Y., and Mehrabzadeh, A. A.: Tropospheric free radical determination by FAGE, Environ. Sci. Technol., 18, 768–777, 1984.

Heard, D. E., Carpenter, L. J., Creasey, D. J., Hopkins, J. R., Lee, J. D., Lewis, A. C., Pilling, M. J., Seakins, P. W., Carslaw, N., and Emmerson, K. M.: High levels of the hydroxyl radical in the winter urban troposphere, Geophys. Res. Lett., 31, doi:10.1029/2004GL020544, 2004.

Kleinman, L. I.: Ozone process insights from field experiments – part II: Observation-based analysis for ozone production, Atmos. Environ., 34, 2023–2033, 2000.

Kovacs, T. A. and Brune, W. H.: Total OH loss rate measurement, J. Atmos. Chem., 39, 105–122, 2001.

Kovacs, T. A., Brune, W. H., Harder, H., Martinez, M., Simpas, J. B., Frost, G. J., Williams, E., Jobson, T., Stroud, C., Young, V., Fried, A., and Wert, B.: Direct measurements of urban OH reactivity during Nashville SOS in summer 1999, J. Environ. Monit., 5, 68–74, doi:10.1039/b204339d, 2003.

Lamb, B., Velasco, E., Allwine, E., Westberg, H., Herndon, S., Knighton, B., Grimsrud, E., Jobson, T., Alexander, M., and Prezeller, P.: Ambient VOC measurements in Mexico City, American Meteorological Society Fifth Conference on Urban Environment, Vancouver, BC, Canada, 23–26 August 2004.

Martinez, M., Harder, H., Kovacs, T. A., Simpas, J. B., Bassis, J., Lesher, R., Brune, W. H., Frost, G. J., Williams, E. J., Stroud, C. A., Jobson, B. T., Roberts, J. M., Hall, S. R., Shetter, R. E., Wert, B., Fried, A., Alicke, B., Stutz, J., Young, V. L., White, A. B., and Zamora, R. J.: OH and HO_2 concentrations, sources, and loss rates during the Southern Oxidants Study in Nashville, Tennessee, summer 1999, J. Geophys. Res., 108, 4617, doi:10.1029/2003JD003551, 2003.

Martinez, M., Harder, H., Brune, W., Di Carlo, P., Williams, E., Hereid, D., Jobson, T., Kuster, W., Roberts, J., Trainer, M., Fehsenfeld, F. C., Hall, S., Shetter, R., Apel, E., Riemer, D., and Geyer, A.: The behavior of the hydroxyl and hydroperoxyl radicals during TexAQS2000, Abstract A12D-0174, AGU Fall Meeting, EOS Transactions, San Francisco, California, 2002.

Molina, L. T. and Molina, M. J. (Ed.): Air Quality in the Mexico Megacity: An integrated assessment, Kluwer Academic Publishers, Boston, 2002.

Mugica, V., Ruiz, M. E., Watson, J., and Chow, J.: Volatile aromatic compounds in Mexico City atmosphere: levels and source apportionment, Atmosfera, 16, 15–27, 2003.

Parrish, D. D., Trainer, M., Young, V., Goldan, P. D., Kuster, W. C., Jobson, B. T., Fehsenfeld, F. C., Lonneman, W. A., Zika, R. D., Farner, C. T., Riemer, D. D., and Rodger, M. O.: Internal consistency test for evaluation of measurements of anthropogenic hydrocarbons in the troposphere, J. Geophys. Res., 103, 22 339–22 359, 1998.

Paulson, S. E., Chung, M. Y., and Hasson, A. S.: OH radical formation from the gas-phase reaction of ozone with terminal alkenes and the relationship between structure and mechanism, J. Phys. Chem. A, 103, 8125–8138, 1999.

Ren, X., Harder, H., Martinez, M., Lesher, R. L., Oliger, A., Shirley, T., Adams, J., Simpas, J. B., and Brune, W. H.: HO_x concentrations and OH reactivity observations during the PMTACS-NY 2001 campaign in New York City, Atmos. Environ., 37, 3627–3637, 2003a.

Ren, X., Harder, H., Martinez, M., Lesher, R. L., Oliger, A., Simpas, J. B., Brune, W. H., Schwab, J. J., Demerjian, K. L., He, Y., Zhou, X., and Gao, H.: OH and HO_2 chemistry in the urban atmosphere of New York City, Atmos. Environ., 37, 3639–3651, 2003b.

Ren, X., Harder, H., Martinez, M., Faloona, I., Tan, D., Lesher, R. L., Di Carlo, P., Simpas, J. B., and Brune, W. H.: Interference testing for atmospheric HO_x measurements by laser-induced fluorescence, J. Atmos. Chem., 47, 169–190, 2004.

Ren, X., Brune, W. H., Cantrell, C. A., Edwards, G. D., Shirley, T., Metcalf, A. R., and Lesher, R. L.: Hydroxyl and peroxy radical chemistry in a rural area of Central Pennsylvania: Observations and model comparisons, J. Atmos. Chem., 52, 231–257, 2005.

Ren, X., Brune, W. H., Oliger, A., Metcalf, A. R., Lesher, R. L., Simpas, J. B., Shirley, T., Schwab, J. J., Bai, C., Li, Y., Demerjian, K. L., and Roychowdhury, U.: OH and HO_2 during the PMTACS–NY Whiteface 2002 Campaign: Observations and Model Comparison, J. Geophys. Res., 111, D10S03, doi:10.1029/2005JD006126, 2006.

Rickard, A. R., Johnson, D., McGill, C. D., and Marston, G.: OH yields in the gas-phase reactions of ozone with alkenes, J. Phys. Chem. A, 103, 7656–7664, 1999.

Sadanaga, Y., Yoshino, A., Kato, S., Yoshioka, A., Watanabe, K., Miyakawa, Y., Hayashi, I., Ichikawa, M., Matsumoto, J., Nishiyama, A., Akiyama, N., Kanaya, Y., and Kajii, Y.: The importance of NO_2 and volatile organic compounds in the urban air from the viewpoint of the OH reactivity, Geophys. Res. Lett., 31, L08102, doi:10.1029/2004GL019661, 2004.

Sander, S. P., Friedl, R. R., Golden, D. M., Kurylo, M. J., Huie, R. E., Orkin, V. L., Moortgat, G. K., Ravishankara, A. R., Kolb, C. E., Molina, M. J., and Finlayson-Pitts, B. J.: Chemical kinetics and photochemical data for use in stratospheric modeling, Evaluation Number 14, JPL Publication 02–25, NASA Jet Propulsion Laboratory, Pasadena, CA, 2003.

Stockwell, W. R., Kirchner, F., and Kuhn, M.: A new mechanism for regional atmospheric chemistry modeling, J. Geophys. Res., 102, 25 847–25 879, 1997.

Velasco, E., Lamb, B., Pressley, S., Allwine, E., Westberg, H., Jobson, T., Alexander, M., Prazeller, P., Molina, L., and Molina, M.: Flux measurements of volatile organic compounds from an urban landscape, Geophys Res. Lett., 32, L20802, doi:10.1029/2005GL023356, 2005.

Volkamer, R., Molina, L. T., Molina, M. J., Shirley, T., and Brune, W. H.: DOAS measurement of glyoxal as an indicator for fast VOC chemistry in urban air, Geophys. Res. Lett., 32, L08806, doi:10.1029/2005GL022616, 2005.

Volz-Thomas, A., Geiss, H., Hofzumahaus, A., and Becker, K.-H.: Introduction to Special Section: Photochemistry Experiment in BERLIOZ, J. Geophys. Res., 108, 8252, doi:10.1029/2001JD002029, 2003.

Volz-Thomas, A., Pätz, H.-W., Houben, N., Konrad, S., Mihelcic, D., Klüpfel, T., and Perner, D.: Inorganic trace gases and peroxy radicals during BERLIOZ at Pabstthum: An investigation of the photostationary state of NO_x and O_3, J. Geophys. Res., 108(D4), 8248, doi:10.1029/2001JD001255, 2003.